Comparing the Active, Functional, and Passive Range of Motion of Finger Joints Using Dynamic Measurement

Yuan, Tianyun; Song, Yu; Goossens, Richard H.M.; Kraan, Gerald A.

DOI
10.1007/978-3-031-32198-6_2

Publication date
2024

Document Version
Final published version

Published in
Convergence

Comparing the Active, Functional, and Passive Range of Motion of Finger Joints Using Dynamic Measurement

Tianyun Yuan, Yu Song, Richard H. M. Goossens, and Gerald A. Kraan

Abstract Studies on finger kinematics, especially the range of motion (RoM) measurements, are essential to understand the use of finger joints and the pathology of related disease. Limited literatures compared the active RoM (A-RoM) of finger joints with either their functional RoM (F-RoM) or passive RoM (p-RoM) using different measuring protocols and tools. This study aims to provide an overall comparison including all three types of RoMs. We measured A-RoM, F-RoM, and P-RoM, using a dynamic measurement system. Our goal is to investigate the relationships among the three RoMs by comparing their extreme rotation angles. The results suggested that P-RoM was the largest motion range, and F-RoM can exceed their A-RoM. The F-RoM of distal-interphalangeal joints may rotated 8–20° more than their A-RoM, mainly during precise and power manipulations. Besides to A-RoM, knowledge of F-RoM and P-RoM are also important for a comprehensive understanding for clinical practice, and thus, to support the optimization and evaluation of treatment devices for finger joint, such as implant replacement.

Keywords 3D motion analysis · Activities of daily living · Finger kinematics

1 Introduction

Range of motion (RoM) is one of the fundamental measurements (Lea and Gerhardt 1995) for studying the biomechanics and kinematics of finger joints. This understanding is crucial to the pathology study and treatment designs for related diseases. However, the significant flexibility of hand fingers challenges the measurement and the study on these joints. There are three types of RoM: active, passive, and functional RoMs (A-RoM, P-RoM, F-RoM). A-RoM presents the maximum motion range

T. Yuan (✉) · Y. Song · R. H. M. Goossens
Delft University of Technology, Delft, The Netherlands
e-mail: T.Yuan@tudelft.nl

G. A. Kraan
Reinier HAGA Orthopaedic Center, Zoetermeer, The Netherlands

M. Melles et al. (eds.), *Convergence: Breaking Down Barriers Between Disciplines*, Springer Series in Design and Innovation 30,
https://doi.org/10.1007/978-3-031-32198-6_2

when the participants perform movements without any assistance; P-RoM is similar to the active one, but it covers the maximum motion range when the participants perform movements with an external force; F-RoM refers to the motion range for the participants to perform a spectrum of activities of daily living.

A great number of articles measured the RoMs of hips and knees during active or loading scenarios (Hemmerich et al. 2006; Kono et al. 2022), and these studies have contributed to the improvement of the implant designs for hips and knees (Mulholland and Wyss 2001; Dennis et al. 1998; Hirata et al. 2015). On the contrary, limited literatures reported the measurement of finger joint RoM, and only several of them compared the A-RoM with either F-RoM or P-RoM (Bain et al. 2015; Gracia-Ibáñez et al. 2017; Hume et al. 1990; Jarque-Bou et al. 2020; Mallon et al. 1991). In addition, these researchers adopted different study protocols and measuring tools. For example, an early study measured the A-RoM and P-RoM of index to small fingers using a goniometer (Mallon et al. 1991), and recent studies utilized a data glove to collect continuous data of finger joints during active and functional hand movements (Gracia-Ibáñez et al. 2017; Jarque-Bou et al. 2020). Most studies concluded that the F-RoM was within the range of the A-RoM (Bain et al. 2015; Gracia-Ibáñez et al. 2017; Hume et al. 1990), but one of the them mentioned that joints extension exceed the A-RoM in some moments of functional activities (Gracia-Ibáñez et al. 2017).

In this study, we aim to challenge the conclusion drawn from current literature by comparing the A-RoM, F-RoM, P-RoM of hand joints. Using an optical tracking system, we continuously measure the rotation angles of target joints during hand activities. Taking the extreme rotations as the boundaries of the RoMs, the initial hypothesis is: the F-RoM is smaller than the A-RoM, and the P-RoM covers both the A-RoM and F-RoM. Since not all three RoMs were combined in one study previously, examining all three ranges in one study can benifit a comprehensive understanding of finger joint movement.

2 Method

2.1 Measuring System

To acquire continuous joint rotation angles through hand activities, we used an optical tracking system with an accuracy 2.7° and a reproducibility 0.8° (Yuan et al. 2022). One part of the system consisted of five RGB cameras (GoPro Inc., San Mateo, CA, USA) which were strategically positioned around the tracking area, as Fig. 1a. All the cameras were in wide-view mode with 5 K (3280 × 2250) resolutions and 30 fps (frame-pre-seconds). The other part of the system consisted of 20 printed ArUco markers attached to the dorsal side of finger segments. ArUco markers are a type of fiducial markers that enable researchers to extract the orientation and the position of each marker in the camera coordinate system from a 2D image (Garrido-Jurado et al. 2014), and thus, to track the movement of each finger segment. The markers were

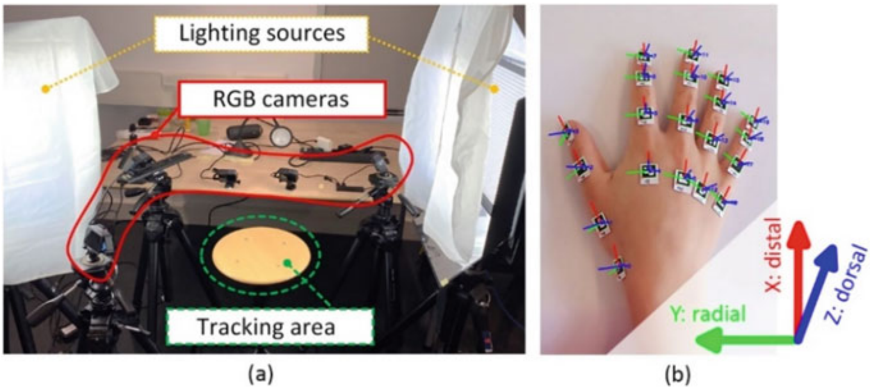

Fig. 1 The applied tracking system. **a** the setup of the cameras and lightening; **b** the marker placement and the corresponding local coordinate system

prepared in three sizes (side length): 7.0 mm, 8.6 mm, and 10.0 mm, for different hand sizes (DINED 2022). During the participation, all markers were coarsely aligned by placing the x-axis of the markers pointing towards the fingertips as Fig. 1b: each marker represented a finger segment.

2.2 *Study Protocol and RoM Definition*

This study included 20 participants (10 males and 10 females) without a history of hand disability or hand surgery. The average age was 31 years (range 21–59 years old). The Human Research Ethical Committee of Delft University of Technology approved this study. All participants signed the consent form before their participation and indicated their right hand as the dominant hand. The sample size was calculated for the two-tailed Wilcoxon signed-rank test (matched pairs) with an effect size of 0.8 and power of 0.9; and this sample size also effects for the one-tailed test with an effect size of 0.8 and power of 0.95 (Faul et al. 2009).

After attaching the markers, participants performed a set of actions in Fig. 2. The figure illustrates some critical posture for the active and passive activities, as well as some potential postures for the functional activities. Action (A1)–(A4) measures the A-RoM, including radial-ulnar (rad-uln) deviation of all fingers, and flexion–extension (flx-ext) of all finger joints. In these actions, we guided the participants to actively bend or rotate their fingers as much as they can. Action (P17)–(P19) also include similar movements, but with an external force applied on the fingers. These actions correspond to the P-RoM. We instructed participants to press the finger segment by themselves and increase the force gradually to the maximum that they can accept to avoid any pain or injury during their participation. Lastly, twelve daily activities were measured for the F-RoM. After comparing the included activities in

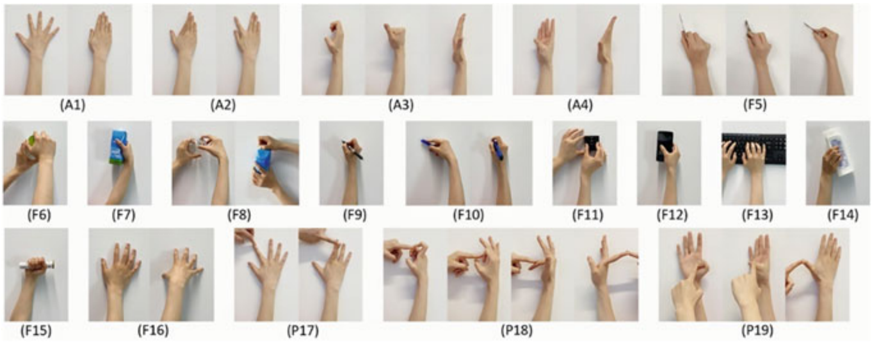

Fig. 2 Illustrations of included activities. Action (A1)–(A4): active activities, action (F5)–(F16): functional activities, action (P17)–(P19): passive activities

previous literature (Bain et al. 2015; Gracia-Ibáñez et al. 2017; Hume et al. 1990; Jarque-Bou et al. 2020; Halilaj et al. 2014), action (F5)–(F12) and (F14)–(F15) were selected to cover the most frequent grasp activities in daily life (Bullock et al. 2013); besides, action (F13) and (F16) represents non-prehensile actions (Dollar 2014).

With the rotation angles of all frames, each type of RoM was defined with the extreme rotation angles of the corresponding actions; from the minimal to the maximum values of the rotation angles.

2.3 Rotation Calculation

We first calculated the rotation of the target joints by extracting the 3D orientations of each marker frame by frame with a self-developed Python program and the OpenCV Library (Yuan et al. 2022). These detected orientations served as the local coordinate system (LCS) for the corresponding finger segments. The analysis included 18 joints: interphalangeal joint (IPJ), metacarpophalangeal joints (MPJ for thumb), and trapeziometacarpal joint (TMCJ) of thumb; distal interphalangeal joint (DIPJ), proximal interphalangeal joint (PIPJ), metacarpophalangeal joint (MCPJ), and carpometacarpal joint (CMCJ) of index to small fingers. Colored markers in Fig. 3a represent the joints, and the numbered squares indicate the markers of the corresponding finger segments. The rotation estimation of a joint was based on two adjacent LCSs: R_{dis} and R_{prx}, which are for the distal and proximal finger segments. For example, the rotation of the TMCJ was calculated from $R_{dis} = R_1$ and $R_{prx} = R_0$. Note that the calculation of the CMCJ of long fingers was relative to the 3rd metacarpal (marker number: 8) (Cooney et al. 1981). For example, the rotation of CMCJ-2 used $R_{dis} = R_4$ and $R_{prx} = R_8$. Here, the CMCJs and TMCJ analyzed in this study were based on the applied simplified kinematic model in Fig. 3a, which is based on but differ from hand anatomy.

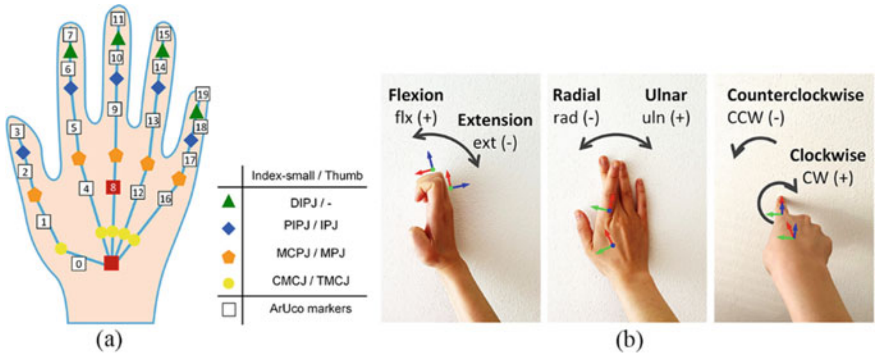

Fig. 3 **a** The applied simplified hand kinematics model and the corresponding markers. **b** The notation and the descriptions of the rotations along the three axes

Knowing the two LCSs, the rotation calculation employed the transformation matrix T in between: $R_{dis} = T R_{prx}$. The rotation angles were the Euler angles following the X–Y–Z sequence as suggested in the ISB (Wu et al. 2005). The positive values indicate flexion, radial deviation, and clockwise rotation (see Fig. 3b).

2.4 Statistical Analysis

With all three types of RoMs: A-RoM, F-RoM, and P-RoM, the normality of the extreme rotation angles of each range was first examined using the Shapiro–Wilk test. Consequently, the matched boundary values were compared using the Wilcoxon signed-rank (two-tailed) test to investigate if there were any differences between these ranges. The null hypothesis was that the extreme rotation angles of any two types of ranges are the same; for example, the maximal flx-ext angles of a joint during active movements is equal to the one during functional activities. Followingly, one-tailed Wilcoxon signed-rank tests were applied to study the relationships among the boundary values. In this study, P-value smaller than 0.05 was considered statistically significant.

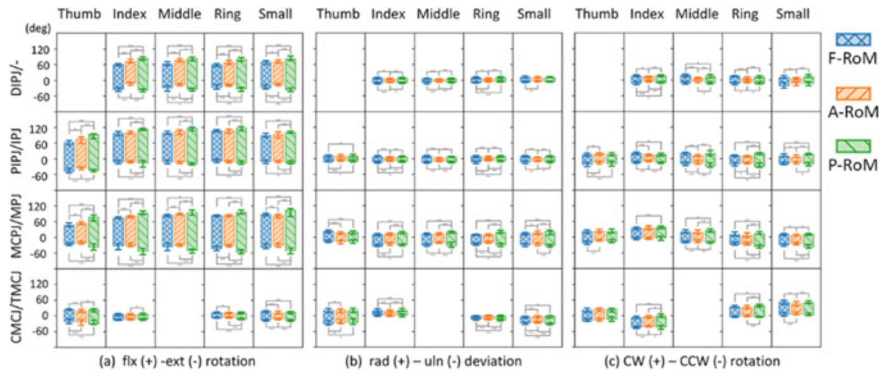

Fig. 4 The medium, 25, and 75 percentiles of the boundaries of the F-RoM, A-RoM, P-RoM of target joints of all participants, and the result of the two-side matched-pair statistical analysis. **a** flexion–extension rotation; **b** ulnar-radial deviation; **c** self-rotation. Vertical unit: degrees. "CW-CC": clockwise – counter-clockwise; "*", "**": the p-value is less than 0.05 or 0.01

3 Results

3.1 The Measured A-RoM, F-RoM, P-RoM

The extreme values of three RoMs along the three rotation axes had 324 sets of boundary values for comparison. The normality analysis of these boundary values suggested that 16% of their distribution failed to fit a normal distribution, and thus, Wilcoxon signed-rank tests was applied in the following statistical analysis.

The corresponding extreme values were compared between any two types of RoMs along each rotation axis (the RoMs of CMCJ-3 were excluded since the 3rd metacarpal bone was used as the reference). The two-tailed analysis suggested statistical differences between A-RoM and P-RoM for most joins as expected. Also, the differences were observed for the flx-ext F-RoM and A-RoM of some joints (see Fig. 4).

3.2 The Difference Among the Three RoMs

The differences between any two types of RoMs were calculated to assess the initial hypothesis: max(F-RoM) < max(A-RoM) < max(P-RoM), and min(F-RoM) > min(A-RoM) > min(P-RoM). Table 1 presents the mean (±SD) of all participants; where positive values support the hypothesis and negative values contrast the initial hypothesis. According to Table 1, larger F-RoM than A-RoM was found in extension, especially for most DIPJ and IPJ; the difference was about 8–20 degrees. Conversely, most differences between maximum boundaries were positive, which means that the functional flexion range was within the active one. The negative differences for rad-uln deviation and self-rotation suggested that F-RoM are larger than the corresponding A-RoM in these rotations. The majority of the difference between A- and P-RoM are positive with statistical significance (see Table 2). Although a few pairs showed slightly negative differences, none of them presented significance. Similarly, no statistical significance was found in the negative differences in Table 3.

4 Discussion

The goal of this study was to compare A-RoM, F-RoM, and P-RoM that measured with continuous data during hand activities. The findings partially agreed with the initial hypothesis, as P-RoM was generally the largest motion range among the three and it covers A-RoM and F-RoM. The measurement in this study were consistent with previous literature (Bain et al. 2015; Gracia-Ibáñez et al. 2017; Hume et al. 1990); however, our F-RoM is larger than theirs, and the findings partially invalidate the hypothesis that A-RoM covers F-RoM.

Comparing the boundaries of F-RoM and A-RoM (see Table 1) revealed that the rotation of hand joints can exceed their A-RoM during functional activities in joint extension, rad-uln deviation, and self-rotation; especially, the differences were pronounced for the extension of MCPJ and DIP/IPJ. This finding disagreed with the conclusion of previous literature (Bain et al. 2015; Gracia-Ibáñez et al. 2017; Hume et al. 1990). The definition of the RoMs can affect the results. In some studies, this phenomenon was mentioned, but the extreme values were excluded (Bain et al. 2015; Gracia-Ibáñez et al. 2017). Differently, we included all possible rotation angles during the functional activities, as these moments may be the key movement for the functional tasks.

The definitions of the A-RoM and P-RoM have little dispute as all studies defined them with the maximum and the minimum rotation angles of the collected data. In contrast, the definition for the F-RoM has two major approaches: (1) take the extreme range of the collected data, (2) use percentiles of the measurement, usually 90% of the extreme range. In this study, we adopted the first approach; we defined all three RoMs with the maximal and minimal rotation angles observed in the data. This method requires high-quality data, because any outliers in the measurement could influence the range. Contrarily, defining RoMs with percentiles of the measurement is more robust, but this can exclude extreme information. For instance, during the performance of a functional task, the duration of the extreme posture with large rotation angles is short, then this only accounts for a small percentage of the full movement and this large rotation angle is excluded. In this study, the extreme rotation angles were included, because although the duration of these hyper-rotations might be short, they are still part of the full activities.

Besides, the measuring approaches can introduce measurement differences among studies. This study applied an optical tracking system to collect continuous data of joint rotation angles and adopted LCS in space in the calculation. The advantage of

Table 1 Differences between F-RoM and A-RoM

	Flexion (Amax-Fmax)	Extension (Fmin-Amin)	Radial (Amax-Fmax)	Ulnar (Fmin-Amin)	CW (Amax-Fmax)	CCW (Fmin-Amin)
TMC-1	−4.8 (±6) *	3.0 (±5) *	−2.6 (±5) *	−4.0 (±8) *	2.0 (±7)	−3.1 (±8)
MP-1	6.0 (±9) *	−5.8 (±13)	−6.9 (±8) *	1.0 (±4)	1.5 (±10)	−9.8 (±7) *
IP-1	7.9 (±15) *	−9.6 (±8) *	0.9 (±4)	−4.0 (±6) *	3.9 (±7) *	−7.9 (±7) *
CMC-2	−1.5 (±5)	−1.6 (±3)	−1.6 (±2) *	1.5 (±4)	1.8 (±4)	−5.6 (±6) *
MCP-2	5.1 (±7) *	−4.5 (±17)	0.8 (±6)	−6.6 (±6) *	1.9 (±7)	−0.6 (±8)
PIP-2	4.6 (±11)	−1.4 (±6)	−3.4 (±4) *	−5.3 (±5) *	−6.3 (±8) *	−6.3 (±6) *
DIP-2	11.6 (±13) *	−20.2 (±13) *	−3.1 (±5) *	−4.9 (±6) *	−4.3 (±8) *	−10.0 (±11) *
CMC-3	/	/	/	/	/	/
MCP-3	5.3 (±7) *	−5.7 (±19)	0.6 (±5)	−10.9 (±9) *	−2.2 (±9)	−4.5 (±6) *
PIP-3	2.9 (±9)	1.6 (±8)	−6.1 (±6) *	−5.3 (±4) *	−9.0 (±6) *	−6.3 (±6) *
DIP-3	12.4 (±8) *	−12.4 (±15) *	−2.5 (±5) *	−3.4 (±6) *	−9.8 (±9) *	−3.4 (±9)
CMC-4	−1.3 (±3) *	−1.4 (±4)	1.1 (±2)	−1.5 (±2) *	−2.1 (±6)	−1.5 (±5)
MCP-4	0.7 (±7)	−10.2 (±13) *	−1.5 (±5)	−6.6 (±5) *	−2.1 (±7)	−1.9 (±10)
PIP-4	−0.6 (±10)	2.9 (±6)	−4.5 (±7) *	−8.4 (±9) *	−3.4 (±8)	−4.0 (±7) *
DIP-4	9.8 (±9) *	−8.4 (±9) *	−2.5 (±6) *	−3.7 (±4) *	−7.9 (±7) *	−3.0 (±9) *
CMC-5	−4.4 (±4) *	−4.5 (±4) *	2.5 (±3) *	−3.4 (±3) *	−4.8 (±9) *	−2.7 (±5) *
MCP-5	−5.6 (±7) *	−5.1 (±12)	3.4 (±5) *	−3.1 (±10)	−2.3 (±11) *	−4.1 (±11)
PIP-5	1.4 (±12)	−0.5 (±4)	−4.4 (±5) *	−4.5 (±6) *	−3.2 (±6) *	−3.5 (±8)
DIP-5	5.1 (±14) *	−8.2 (±9) *	−1.9 (±8)	−2.2 (±7) *	−4.2 (±7) *	−4.0 (±15)

*: p-value < 0.05

Table 2 Differences between A-RoM and P-RoM

	Flexion (Pmax-Amax)	Extension (Amin-Pmin)	Radial (Pmax-Amax)	Ulnar (Amin-Pmin)	CW (Pmax-Amax)	CCW (Amin-Pmin)
TMC-1	4.2 (±9) *	1.4 (±4)	3.3 (±8)	−0.7 (±9)	−0.2 (±7)	0.9 (±9)
MP-1	18.7 (±13) *	17.9 (±16) *	1.4 (±8)	−1.3 (±4)	−0.1 (±11)	4.4 (±11)
IP-1	13.6 (±18) *	8.9 (±9) *	1.3 (±5)	1.8 (±4)	−1.0 (±8)	1.9 (±8)
CMC-2	2.0 (±3) *	1.8 (±7)	3.6 (±4) *	−0.5 (±5)	3.5 (±5) *	3.6 (±6) *
MCP-2	11.5 (±21) *	23.7 (±12) *	6.0 (±4) *	3.3 (±8)	3.1 (±9)	−1.1 (±5)
PIP-2	11.5 (±7) *	8.1 (±10) *	2.4 (±3) *	3.0 (±2) *	1.7 (±5)	6.9 (±6) *
DIP-2	9.9 (±8) *	24.2 (±10) *	2.6 (±3) *	3.2 (±6) *	5.4 (±8) *	4.8 (±4) *
CMC-3	/	/	/	/	/	/
MCP-3	5.4 (±23) *	21.7 (±9) *	7.0 (±5) *	10.0 (±9) *	7.1 (±11) *	4.8 (±6) *
PIP-3	11.8 (±10) *	7.4 (±7) *	4.6 (±8) *	4.0 (±5) *	9.7 (±7) *	10.0 (±8) *
DIP-3	3.0 (±15) *	17.2 (±14) *	4.1 (±6) *	2.7 (±4) *	7.3 (±7) *	5.1 (±11) *
CMC-4	0.4 (±3)	5.7 (±4) *	−0.9 (±2)	3.2 (±3) *	7.6 (±8) *	4.1 (±6) *
MCP-4	12.2 (±20) *	22.0 (±10) *	11.2 (±8) *	10.9 (±7) *	7.8 (±8) *	10.9 (±11) *
PIP-4	9.0 (±11) *	5.2 (±6) *	5.1 (±8) *	3.6 (±5) *	11.3 (±7) *	10.6 (±10) *
DIP-4	8.0 (±15) *	15.7 (±9) *	2.9 (±4) *	1.0 (±3)	8.1 (±11) *	2.5 (±5) *
CMC-5	1.5 (±5)	6.1 (±3) *	−0.0 (±2)	5.5 (±6) *	6.8 (±8) *	1.5 (±6)
MCP-5	15.3 (±23) *	20.5 (±16) *	3.4 (±4) *	4.8 (±6) *	2.2 (±10) *	10.2 (±10) *
PIP-5	9.9 (±10) *	3.6 (±4) *	3.7 (±5) *	2.4 (±4) *	8.4 (±7) *	4.7 (±9) *
DIP-5	13.1 (±15) *	18.7 (±11) *	1.8 (±8)	0.7 (±8)	7.2 (±10) *	−0.7 (±13)

*: p-value < 0.05

Table 3 Differences between F-RoM and P-RoM

	Flexion (Pmax-Fmax)	Extension (Fmin-Pmin)	Radial (Pmax-Fmax)	Ulnar (Fmin-Pmin)	CW (Pmax-Fmax)	CCW (Fmin-Pmin)
TMC-1	−0.6 (±9)	4.4 (±6) *	0.7 (±7)	−4.8 (±9) *	1.8 (±9)	−2.2 (±10)
MP-1	24.6 (±16) *	12.1 (±14) *	−5.5 (±6) *	−0.3 (±6)	1.4 (±11)	−5.3 (±12)
IP-1	21.5 (±22) *	−0.6 (±7)	2.2 (±4) *	−2.1 (±5) *	2.9 (±7)	−6.0 (±9) *
CMC-2	0.6 (±4)	0.2 (±7)	2.0 (±3) *	1.0 (±4)	5.3 (±6) *	−2.0 (±7)
MCP-2	16.7 (±21) *	19.2 (±19) *	6.8 (±6) *	−3.3 (±6) *	5.0 (±9) *	−1.7 (±9)
PIP-2	16.1 (±9) *	6.7 (±8) *	−1.0 (±4)	−2.3 (±5) *	−4.6 (±7) *	0.6 (±6)
DIP-2	21.5 (±13) *	3.9 (±8)	−0.5 (±4)	−1.7 (±5)	1.1 (±7)	−5.1 (±11) *
CMC-3	/	/	/	/	/	/
MCP-3	10.8 (±21) *	15.9 (±21) *	7.6 (±6) *	−0.9 (±11)	4.9 (±10) *	0.3 (±6)
PIP-3	14.8 (±11) *	9.0 (±9) *	−1.4 (±9)	−1.3 (±4)	0.7 (±10)	3.7 (±10)
DIP-3	15.4 (±17) *	4.9 (±7) *	1.6 (±7)	−0.6 (±5)	−2.5 (±5) *	1.7 (±7)
CMC-4	−0.9 (±3)	4.3 (±5) *	0.2 (±3)	1.6 (±2) *	5.5 (±10) *	2.6 (±7)
MCP-4	12.9 (±19) *	11.8 (±15) *	9.7 (±8) *	4.3 (±8) *	5.7 (±7) *	9.1 (±8) *
PIP-4	8.5 (±10) *	8.1 (±6) *	0.7 (±8)	−4.8 (±9) *	7.9 (±6) *	6.6 (±10) *
DIP-4	17.8 (±14) *	7.4 (±11) *	0.4 (±6)	−2.7 (±5) *	0.2 (±11)	−0.5 (±5)
CMC-5	−3.0 (±3) *	1.6 (±5)	2.4 (±4) *	2.1 (±4) *	2.0 (±11)	−1.1 (±7)
MCP-5	9.7 (±21) *	15.3 (±10) *	6.8 (±6) *	1.7 (±8)	−0.1 (±7)	6.2 (±8) *
PIP-5	11.3 (±11) *	3.1 (±5) *	−0.7 (±6)	−2.1 (±7)	5.2 (±7) *	1.2 (±11)
DIP-5	18.2 (±10) *	10.5 (±12) *	−0.1 (±5)	−1.5 (±8)	3.0 (±9)	−4.8 (±11)

*: p-value < 0.05

our system was that the rotations of all finger joints can be measured simultaneously, and all joints were considered as three degrees of freedom joints. In comparison, studies using (electro-) goniometers or flex sensors assumed the joint as a one degree of freedom joint, which is in contrast to the anatomy. The measured RoM of our study was consistent with another study that also calculated the rotation angles of finger joints along three axes using captured LCS (Coupier et al. 2016). We both found that self-rotation coupled with flx-ext and rad-uln deviation. The detected self-rotation and rad-uln deviation indicated that certain torque was applied on the joints during movements, as detailed in an in-vivo study that underlined the importance of self-rotation when considering the joint rotations of fingers (Degeorges and Oberlin 2003). With the accessibility to advance devices and techniques, we encourage considering the joints as three degrees of freedom in the measurement and analysis.

Moreover, the selection of the functional activities may also influence the results. In selecting the functional activities, we intended to include both prehensile and non-prehensile activities instead of focusing on the prehensile movement only. The reason was that the prehensile actions are mainly accomplished with finger flexion, then the extension will be excluded. The selected 12 activities in the present study tried to cover more scenarios for the activities of daily living. The moments with hyper-rotation occurred mainly during fine manipulation or power grasp, when the force was crucial for controlling the object with fingers or stabilizing the object within the hand. For example, key pinch for opening the door or press for pushing objects. The reaction force during the interaction between the fingers and the object may increase the rotation ranges.

The two main limitations of this study were the sample size and the intervention of a nature movement. Although the number of included participants was adequate for matched-pair comparisons, increasing the sample size may enable detailed statistical analysis related to gender, handiness, and hand size (Mallon et al. 1991). The applied optical tracking system was a marker-based system. Marker loosening was observed when participants with small hands performed some functional activities and those frames were excluded. To avoid such issue and record more nature movements in the future, marker-less tracking system can be an option (Geelen et al. 2021). Nonetheless, these systems currently are less robust than marker-based systems and they require a larger database for training and ensuring the tracking accuracy (Yuan et al. 2017).

This study suggested that A-RoM had a large overlap but was unable to cover the range for some functional activities. Thus, the studying the F-RoM and P-RoM are as important as the A-RoM for a comprehensive understanding of the kinematics of hand joints. The knowledge of all three types of RoMs can support clinical diagnosis and treatment, also, it can contribute to the optimization and evaluation of the hand-related designs, such as implant designs for fingers or hand splints.

References

Bain GI, Polites N, Higgs BG, Heptinstall RJ, McGrath AM (2015) The functional range of motion of the finger joints. J Hand Surg (european Volume) 40(4):406–411

Bullock IM, Zheng JZ, De La Rosa S, Guertler C, Dollar AM (2013) Grasp frequency and usage in daily household and machine shop tasks. IEEE Trans Haptics 6(3):296–308

Cooney WP, Lucca MJ, Chao EY, Linscheid RL (1981) The kinesiology of the thumb trapeziometacarpal joint. J Bone Joint Surg Am 63(9):1371–1381

Coupier J, Hamoudi S, Telese-Izzi S, Feipel V, Rooze M, Jan SVS (2016) A novel method for in-vivo evaluation of finger kinematics including definition of healthy motion patterns. Clin Biomech 31:47–58

Degeorges R, Oberlin C (2003) Measurement of three-joint-finger motions: reality or fancy? A three-dimensional anatomical approach. Surg Radiol Anat 25(2):105–112

Dennis DA, Komistek RD, Stiehl JB, Walker SA, Dennis KN (1998) Range of motion after total knee arthroplasty The effect of implant design and weight-bearing conditions. J Arthroplasty 13(7):748–752

DINED, https://dined.io.tudelft.nl/en/database/tool. Accessed 01 Oct 2022

Dollar AM (2014) Classifying human hand use and the activities of daily living. In: The human hand as an inspiration for robot hand development. Springer

Faul F, Erdfelder E, Buchner A, Lang AG (2009) Statistical power analyses using G* Power 3.1: tests for correlation and regression analyses. Behav Res Methods 41(4):1149–1160

Garrido-Jurado S, Muñoz-Salinas R, Madrid-Cuevas FJ, Marín-Jiménez MJ (2014) Automatic generation and detection of highly reliable fiducial markers under occlusion. Pattern Recogn 47(6):2280–2292

Geelen JE, Branco MP, Ramsey NF, Van Der Helm FC, Mugge W, Schouten AC (2021) MarkerLess motion capture: ML-MoCap, a low-cost modular multi-camera setup. In: 2021 43rd annual international conference of the IEEE engineering in medicine & biology society (EMBC), pp 4859–4862

Gracia-Ibáñez V, Vergara M, Sancho-Bru JL, Mora MC, Piqueras C (2017) Functional range of motion of the hand joints in activities of the international classification of functioning, disability and health. J Hand Ther 30(3):337–347

Halilaj E, Rainbow MJ, Got C, Schwartz JB, Moore DC, Weiss APC, Ladd AL, Crisco JJ (2014) In vivo kinematics of the thumb carpometacarpal joint during three isometric functional tasks. Clin Orthop Relat Res 472(4):1114–1122

Hemmerich A, Brown H, Smith S, Marthandam SSK, Wyss UP (2006) Hip, knee, and ankle kinematics of high range of motion activities of daily living. J Orthop Res 24(4):770–781

Hirata M, Nakashima Y, Hara D, Kanazawa M, Kohno Y, Yoshimoto K, Iwamoto Y (2015) Optimal anterior femoral offset for functional range of motion in total hip arthroplasty—a computer simulation study. Int Orthop 39(4):645–651

Hume MC, Gellman H, McKellop H, Brumfield RH Jr (1990) Functional range of motion of the joints of the hand. J Hand Surg 15(2):240–243

Jarque-Bou NJ, Atzori M, Müller H (2020) A large calibrated database of hand movements and grasps kinematics. Sci Data 7(1):1–10

Kono K, Inui H, Tomita T, Yamazaki T, Taketomi S, Yamagami R, Kawaguchi K, Kage T, Arakawa T, Tanaka S (2022) Effect of weight-bearing in bicruciate-retaining total knee arthroplasty during high-flexion activities. Clin Biomech 92:105569

Lea RD, Gerhardt JJ (1995) Range-of-motion measurements. J Bone Joint Surg Am 77(5):784–798

Mallon WJ, Brown HR, Nunley JA (1991) Digital ranges of motion: normal values in young adults. J Hand Surg 16(5):882–887

Mulholland SJ, Wyss UP (2001) Activities of daily living in non-Western cultures: range of motion requirements for hip and knee joint implants. Int J Rehabil Res 24(3):191–198

Wu G, Van der Helm FC, Veeger HD, Makhsous M, Van Roy P, Anglin C, Nagels J, Karduna AR, McQuade K, Wang X, Werner FW (2005) ISB recommendation on definitions of joint coordinate systems of various joints for the reporting of human joint motion—Part II: shoulder, elbow, wrist and hand. J Biomech 38(5):981–992

Yuan S, Ye Q, Stenger B, Jain S, Kim TK (2017) Bighand2. 2m benchmark: hand pose dataset and state of the art analysis. In: Proceedings of the IEEE conference on computer vision and pattern recognition, pp 4866–4874

Yuan T, Song Y, Kraan GA, Goossens RH (2022) Identify finger rotation angles with ArUco markers and action cameras. J Comput Inf Sci Eng 22(3):031011